Semiactive Suspension Design With An Optimal Gain Switching Target

Alessandro Giua, Carla Seatzu, Giampaolo Usai

DIEE, Università di Cagliari, Piazza d'Armi, 09123 Cagliari, Italy

email: giua@diee.unica.it, tel: +39 070 675.58.92, fax: +39 070 675.59.00

Abstract

The paper presents a two-phase design technique for semiactive suspensions. In the first phase, we use a procedure proposed by Yoshida et al. to compute a target active control law that can be implemented by Optimal Gain Switching. This control law is such that the force generated by the suspension system is bounded within a set U. In the second phase, we approximate this target by controlling the damper coefficient of the semiactive suspension. We also compute the region of the state space in which the force generated by the semiactive suspension is still within the set U. The results of several simulations show that the use of a semiactive suspension leads to minimal loss with respect to optimal performance of an active suspension.

Published as:

A.Giua, C.Seatzu, G. Usai, "Semiactive Suspension Design With An Optimal Gain Switching Target", Vehicle System Dynamics, Vol. 31, No. 4, pp. 213- 232, April, 1999.

1 Introduction

The design of active suspensions for road vehicles aims to optimize the performance of the vehicle with regard to comfort, road holding, and rideability.

In an active suspension there are no passive elements, such as dampers and springs. The interaction between vehicle body and wheel is regulated by an actuator of variable length. The actuator is usually hydraulically controlled and applies between body and wheel a force that represents the control action generally determined with an optimization procedure.

Active suspensions [3, 8, 14] have better performance than passive suspensions. However, active suspension systems are rather complex, since they require several components such as actuators, servovalves, high-pressure tanks for the control fluid, sensors for detecting the system state, etc. The associated power, that must be provided by the vehicle engine, may reach the order of several 10 kW [6] depending on the required performance. Furthermore, these suspension systems have a high cost.

As a viable alternative to a purely active suspension system, the use of semiactive suspensions has been considered [1, 4, 6, 7, 9, 12]. Such a system consists of a spring whose stiffness is constant and of a damper whose characteristic coefficient f can be made to change within an interval $[f_{\min}, f_{\max}]$ controlling the opening of a valve. The time required to update f is usually less than 10^{-2}s.

A semiactive suspension is a valid engineering solution when it can reasonably approximate the performance of the active control. In fact, a semiactive suspension requires a low power controller than can be easily realized at a lower cost than that of a fully active one. In general, a semiactive suspension design consists of two phases [1]:

- Design a good active law, $u(\cdot)$ to be considered as a "target".
- Design the semiactive suspension so that its control law $u_s(\cdot)$ approximates as close as possible the target law.

In the following two subsections, we discuss in detail these two phases.

1.1 Target active law

Thompson [14] was the first to explore the use of optimal control techniques to design an active law so as to minimize a performance index of the form $J = \sum_{k=0}^{\infty} x^T(k)Qx(k) + ru^2(k)$, where x is the system state and u the control force provided by the actuator. This design technique is called LQR [10, 11] and has also been used by other authors [1, 3, 12]. Its two main advantages are: a) the optimal solution can be easily computed solving a Riccati equation; b) it takes the form of a state feedback law with constant gains.

We observe that the performance of a suspension system is related to the minimization of the term x^TQx. The presence of the term ru^2 imposes a penalty on the magnitude of the control force but cannot limit its maximal value within a given bound.

In this paper, we present a design technique in which we assume as optimal the control law $u^*(\cdot)$ that minimizes a performance index of the form $J = \sum_{k=0}^{\infty} x^T(k)Qx(k)$ under the constraint $|u(k)| \leq u_{\max}$. The minimization of this index with a suitable choice of Q leads to a good performance. The constraint on the control input bounds the acceleration of the sprung mass — at least in nominal operating conditions, i.e., when the linear model of the suspension is valid — so as to ensure the comfort of the passengers. Furthermore, this constraint limits the maximal force required from the controller, i.e., it leads to the choice of a suitable actuator.

The main problem with this approach is that in general the law $u^*(\cdot)$ cannot be implemented as a feedback law with constant gains and that it is difficult to compute [15]. Thus its implementation in an on-board controller is unfeasible.

Yoshida *et al.* [16] have proposed, however, a methodology to approximate this law by means of an adaptive controller that switches between different constant state feedback gains. Each K_ρ is the state feedback gain that gives the optimal feedback law that minimizes a performance index of the form $J_\rho = \sum_{k=0}^{\infty} \rho x^T(k)Qx(k) + ru^2(k)$, where the weight ρ belongs to a finite discrete set. We call this law Optimal Gain Switching (OGS) and denote it by $u_{OGS}(\cdot)$. Yoshida provides a simple algorithm for choosing the suitable weight ρ as a function of the present system state while always ensuring that $|u_{OGS}(k)| \leq u_{\max}$ holds. When the system state is far from the origin a small ρ is selected, while for small disturbances a large ρ may be used.

The results of numerical simulations [13], show that for the case of a quarter car sus-

pension the active control laws $u^*(\cdot)$ and $u_{OGS}(\cdot)$ are very similar and the corresponding responses of the suspension system are also almost identical. When compared with the LQR controller, the OGS controller has two fundamental advantages. Firstly, it ensures a bound on the magnitude of the force that the actuator needs to provide. Secondly, while the LQR controller realizes a particular trade-off between performance (term x^TQx) and comfort (term ru^2), the OGS controller adapts the trade-off to different road conditions and car velocities, applying different control laws depending on the magnitude of the disturbance.

1.2 Semiactive approximation

On the base on the previous analysis, we propose to choose as target for the semiactive control law $u_s(\cdot)$ the law $u_{OGS}(\cdot)$. At each sampling instant k the controller should select the damper coefficent f in the set $[f_{\min}, f_{\max}]$ so as to minimize $(u_{OGS}(k) - u_s(k))^2$. In this case it may happen that the condition $|u_s(k)| \leq u_{\max}$ is violated. We show how to compute the state space region in which this condition holds, and we see that in practical cases this region is large enough to contain most of all possible evolutions of the system.

Finally we compare the performance of the semiactive suspension system with that of an active suspension that implements the OGS controller. Different simulations have been carried out, considering the presence of input disturbances caused by the road profile or the presence of initial conditions on the state. The results of these simulations show that the semiactive suspension performes reasonably well, and is a good approximation of the active suspension.

The semiactive control law we derive in this paper can be implemented with standard tools of today technology. The control algorithm requires simple computations that a modern microprocessor is capable of executing within the sampling period we have chosen (10^{-2}s). The computation of the semiactive law requires the knowledge of the system's state. Although not all state variables (and the external disturbance is also a state variable) can be measured, the system is observable and thus an observer can be designed to estimate all state variables. We briefly comment on this point, but the design of an observer is not addressed in this paper.

1.3 Advantages of an adaptive suspension

The choice of the OGS law as a target, leads to a suspension control law that changes to "optimally" adapt to different road conditions.

The need for adaptive suspensions is deeply felt in many applications such as Sport Utility Vehicles (SUV), a class of vehicles that is gaining more and more market shares both in USA and Europe. It is desirable that such a vehicle behaves as a normal car on-road, while offering the same performance of a off-road vehicle on a rough profile.

These requirements can be expressed as follows.

In nominal conditions on-road (small disturbances) the suspension control law should lead to energic actions to keep the asset. In practice, this corresponds to a choice of a damper coefficient f close to $f_{\max}$.

Off-road, on the contrary, the suspension system is subject to high suspension deformation and high deformation velocity. To avoid excessive forces, a choice of a damper coefficient f close to $f_{\min}$ is suitable.

The approach prosed in this paper answers to this need, because it leads to design a suspension that is not too soft for small disturbances, and not too stiff for large disturbances.

We stress that this control law should only be operative during nominal conditions, and not in emergency conditions when the vehicle is subject to abrupt changes in direction and velocity. In this case, of course, the control law we propose could be excluded and the $f_{\max}$ value for the damper coefficient should be chosen by a standard safety system, as already existing on many commercial vehicles.

A similar approach was also presented in [5] where a modified OGS technique was used to design a tandem active-passive suspension systems. In this design two constraints on the control force were considered: both the total force applied between wheel and body, and the fraction of the force generated by the actuator should never exceed given bounds. The new constraint on the active force leads to the dimensioning of a suitable actuator to be added in parallel to the passive suspension.

This paper is structured as follows. In Section 2 we present the dynamical model of the quarter car suspension system considered in this work. In Section 3 we recall the OGS control design as presented by Yoshida. In Section 4 we show how it is possible to

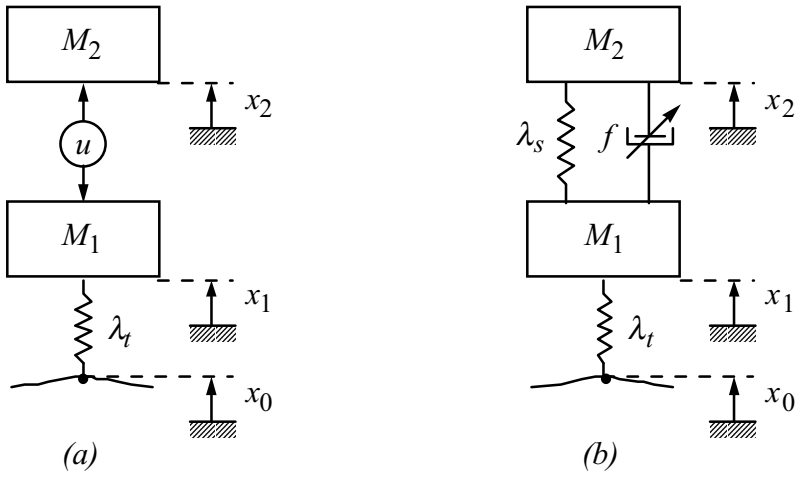

Figure 1: *Scheme of two degree-of-freedom suspension: (a) active suspension; (b) semiactive suspension.*

approximate the OGS law with a semiactive suspension. We also define the state space region in which the semiactive force is garanteed to never exceed the bound $u_{\max}$. In Section 5 we present the results of three different simulations. In Appendix we present and prove a lemma that gives necessary and sufficient conditions for deriving the state space region in which the semiactive law, that approximates an active law bounded to be in U, is still within U.

2 Dynamical model of the suspension system

We refer to the suspension with two degrees of freedom schematized in Figure 1.a). We used the following notation:

- M_1 is the equivalent nonsprung mass consisting of the wheel and its moving parts;
- M_2 is the sprung mass, i.e., the part of the whole body mass and the load mass pertaining to only one wheel;
- $x_1(t)$ is the nonsprung mass displacement at time t with respect to a fixed reference;
- $x_2(t)$ is the displacement of the sprung mass with respect to the same fixed reference;
- $x_3(t) = \dot{x}_1(t)$ is the velocity of the nonsprung mass;

- $x_4(t) = \dot{x}_2(t)$ is the velocity of the sprung mass;
- λ_t is the elastic constant of the tire, whose damping characteristics have been neglected. This is in line with almost all researchers who have investigated synthesis of active suspensions for motor vehicles as the tire damping is minimal;
- $u(t)$ is the control action, i.e., the force produced by the actuator;
- $x_0(t)$ is the function representing the disturbance, which simulates the longitudinal profile of the road.

It is readily shown that the state variable mathematical model of the system under study is given by

$$\dot{x}(t) = Ax(t) + Bu(t) + Lx_0(t) \tag{1}$$

where $x(t) = [x_1(t)x_2(t)x_3(t)x_4(t)]^T$ is the state, whereas the constant matrices A, B and L have the following structure:

$$A = \begin{bmatrix} 0 & 0 & 1 & 0 \\ 0 & 0 & 0 & 1 \\ -\frac{\lambda_t}{M_1} & 0 & 0 & 0 \\ 0 & 0 & 0 & 0 \end{bmatrix}; B = \begin{bmatrix} 0 \\ 0 \\ -\frac{1}{M_1} \\ -\frac{1}{M_2} \end{bmatrix}; L = \begin{bmatrix} 0 \\ 0 \\ -\frac{\lambda_t}{M_1} \\ 0 \end{bmatrix}.$$

The disturbance $x_0(t)$ that takes into account the longitudinal road profile and also depends on vehicle speed is assumed to be stochastic and may be characterized by its power spectral density (PSD) distribution function.

Here, the road roughness characteristics are expressed by a signal whose PSD distribution function is [8]

$$\Phi(\omega) = \frac{cV}{\omega^2 + \alpha^2 V^2} \tag{2}$$

where $c = (\sigma^2/\pi)\alpha$. σ^2 denotes the road roughness variance and V the vehicle speed, whereas the coefficients c and α depend on the type of road surface. The product is the power spectrum of the white noise.

The signal $x_0(t)$, whose PSD is given by (2), may be obtained as the output of a linear filter expressed by the differential equation

$$\dot{x_0}(t) = -\alpha V x_0(t) + w(t). \tag{3}$$

The problem of stochastic optimal control is usually formulated considering an augmented system whose state variables also contain $x_0(t)$ while the disturbance is represented by the white noise $w(t)$.

Let $x_0(t) = x_5(t)$ and by taking into account (3), the augmented system is [3]

$$\dot{\tilde{x}}(t) = \tilde{A}\tilde{x}(t) + \tilde{B}u(t) + \tilde{L}w(t) \tag{4}$$

where $\tilde{x}(t) = [x_1(t)x_2(t)x_3(t)x_4(t)x_5(t)]^T$ and

$$\tilde{A} = \begin{bmatrix} A & L \\ 0 & -\alpha V \end{bmatrix}; \tilde{B} = \begin{bmatrix} B \\ 0 \end{bmatrix}; \tilde{L} = \begin{bmatrix} 0 \\ 1 \end{bmatrix}.$$

The pair (A, B) is completely controllable, and the filter represented by (3) is asymptotically stable ($\alpha V > 0$); therefore, the pair $(\tilde{A}, \tilde{B})$ is stabilizable.

The control law we will design in the following sections requires the knowledge of the system state $\tilde{x}$. Since not every component of $\tilde{x}(t)$ is directly measurable, we reconstruct the state through an appropriate state observer. To do this, we choose a suitable matrix $\tilde{C}$ for the output equation

$$y(t) = \tilde{C}\tilde{x}(t). \tag{5}$$

If we assume [3]

$$\tilde{C} = \begin{bmatrix} 1 & -1 & 0 & 0 & 0 \\ 0 & 0 & 0 & 1 & 0 \end{bmatrix} \tag{6}$$

which correspond to measuring the suspension deformation and the sprung mass velocity, the observability of the pair $(\tilde{A}, \tilde{C})$ is ensured.

The control approach we will follow, makes use of a discrete-time state space model. Thus we choose a sampling interval T and discretize equation (4) to obtain [11]

$$\tilde{x}(k+1) = G\tilde{x}(k) + Hu(k) + Ww(k) \tag{7}$$

where

$$G = e^{\tilde{A}T}; \quad H = \left(\int_0^T e^{\tilde{A}\tau} d\tau\right) \tilde{B}; \quad W = \left(\int_0^T e^{\tilde{A}\tau} d\tau\right) \tilde{L}.$$

It is known [11] that a system that is stabilizable and observable in the absence of sampling maintains these properties after the introduction of sampling if and only if, for every eigenvalue of the characteristic equation for the continuous-time control system, the relationship

$$Re\{\lambda_i\} = Re\{\lambda_j\} \tag{8}$$

implies

$$Im\{\lambda_i - \lambda_j\} \neq \frac{2n\pi}{T} \quad n = \pm 1, \pm 2, \ldots . \tag{9}$$

In the actual case the set of eigenvalues of $\tilde{A}$ are:

$$\left\{ -\alpha V, \quad 0, \quad 0, \quad i\left(\frac{\lambda_t}{M_1}\right)^{1/2}, \quad -i\left(\frac{\lambda_t}{M_1}\right)^{1/2} \right\}$$

so it is necessary to choose a sampling period T, such that:

$$T \neq n\pi \left(\frac{M_1}{\lambda_t}\right)^{1/2} . \tag{10}$$

3 OGS design of an active suspension

The design of the active suspension requires determining a suitable control law $u(\cdot)$ for system (7).

We consider as target the control law $u^*(\cdot)$ that minimizes a performance index of the form:

$$J = \sum_{k=0}^{\infty} \tilde{x}^T(k) Q \tilde{x}(k), \tag{11}$$

(with Q positive semidefinite) under constraint (7) and constraint

$$|u(k)| \leq u_{\max} \qquad (k \geq 0). \tag{12}$$

It is well known [15] that the optimal solution $u^*(\cdot)$ does not correspond in general to a feedback control law and furthermore its computation is quite burdensome.

Yoshida *et al.* [16] have proposed a simple procedure that well approximates the optimal control law $u^*(\cdot)$ by switching among feedback control laws whose gains can be computed as solution of a family of LQR problems. We call this procedure *Optimal Gain Switching* (OGS) and the corresponding feedback law will be denoted $u_{\mathrm{OGS}}(\cdot)$.

Here we briefly outline the OGS procedure. Let us consider a family of performance indexes

$$J_\rho = \sum_{k=0}^{\infty} \left[\rho \tilde{x}^T(k) Q \tilde{x}(k) + r u^2(k)\right] . \tag{13}$$

For a given value of ρ the unconstrained control law $u_\rho(\cdot)$ that minimizes J_ρ can be written as

$$u_\rho(k) = -K_\rho \tilde{x}(k)$$

where the gain matrix K_ρ can be computed by solving an algebraic Riccati equation [10].

Furthermore, for a given value of ρ it is possible to compute a *linear region* Γ_ρ in the state space such that for any point $\tilde{x}_0$ within this region the following equation holds:

$$|u_\rho(k)| \equiv |K_\rho \hat{G}_\rho^k \tilde{x}_0| \leq u_{\max}, \qquad (k \geq 0) \tag{14}$$

where $\hat{G}_\rho = G - HK_\rho$. Thus, if we consider the system (7) with input noise $w(k) = 0$, feedback law u_ρ and an initial state $\tilde{x}_0 \in \Gamma_\rho$ we can be sure that in its future evolution the value of the control input will always satisfy equation (12).

Yoshida has shown that it is possible to determine suitable matrices Z_ρ such that $\tilde{x}_0 \in \Gamma_\rho$ if and only if $-\vec{u}_{\max} \leq Z_\rho \tilde{x}_0 \leq \vec{u}_{\max}$, where $\vec{u}_{\max}$ is a column vector whose components are all equal to $u_{\max}$. In effect,

$$Z_\rho = \begin{bmatrix} K_\rho \\ K_\rho \hat{G}_\rho \\ \vdots \\ K_\rho \hat{G}_\rho^{j_\rho} \end{bmatrix}$$

so we only need to verify equation (14) for the first $j_\rho + 1$ sampling instants. The value of j_ρ is a function of ρ and can be computed solving a linear programming problem.

The control procedure consists of two phases.

During the *off-line phase*, we choose a finite set of m values for ρ, namely $\{\rho_1, \cdots, \rho_m\}$. For each ρ_i we compute the corresponding gain matrix K_{ρ_i} and the linear region matrix Z_{ρ_i}.

During the *on-line* phase, at each sampling instant $k \geq 0$ we choose a suitable gain. This requires measuring the present state $\tilde{x}(k)$, and determining $\rho(k) \equiv \max\{\rho_i \mid \tilde{x}(k) \in \Gamma_{\rho_i}\}$. The suitable feedback gain to be applied at time instant k is then $K_{\rho(k)}$, i.e., we choose

$$u_{\mathrm{OGS}}(k) = -K_{\rho(k)} \tilde{x}(k). \tag{15}$$

It has been shown by Yoshida that if no disturbance is acting on the system, then $\rho(k)$ is a nondecreasing function of k. This is not the case, however, in the model given by (7),

because of the presence of $w(k)$. Thus, in general it may be necessary at a given sampling instant, to switch from one value of ρ to a smaller one.

It is important to highlight the advantages and limits of the OGS control scheme.

It has been shown by Yoshida that the control law $u_{\mathrm{OGS}}(\cdot)$ leads to values of the performance index (11) that are close the absolute minimum given by the optimal control law $u^*(\cdot)$. Furthermore in [13] it was shown that the performance in terms of state evolution, resulting from the two laws are very close. Thus, we think that the OGS control law gives a very good feedback approximation of the optimal law.

In [13] it was noted that a good choice of the values ρ_i may influence the performance of the OGS law. As m increases, the approximation is better, but the procedure becomes computationally more intensive.

The computational complexity of the OGS control law requires some comments. The most burdensome part of this procedure is the off-line phase, where the matrices Z_{ρ_i} are computed. During the on-line phase, it is necessary at each sampling instant k to compute at most m matrix products $Z_{\rho_i}\tilde{x}(k)$. The number of rows of the different Z_{ρ_i} is not constant and is equal to $j_{\rho_i}+1$. In Section 5, we will discuss the number of elementary operations required to compute the OGS control law at each sampling instant.

4 Semiactive approximation of the OGS law

In this section we show how the OGS law, that requires an actuator, may be approximated by a semiactive suspension, whose varying parameter is the characteristic coefficient of the damper f.

In Figure 1.b, we have represented a conventional semiactive suspension composed of a spring with elastic constant λ_s, and of a damper with adaptive characteristic coefficient f.

The effect of this suspension is equivalent [3] to that of a control force

$$u_s(k) = [\ \lambda_s \quad -\lambda_s \quad +f \quad -f \quad 0\ ]\tilde{x}(k). \tag{16}$$

Note that, as f may vary, $u_s(k)$ is both a function of f and of $\tilde{x}(k)$.

In general, f can only take values in a real set $[f_{\min}, f_{\max}]$. We propose to choose at each

step k the value of $f(k)$ to minimize the difference

$$F[f, \tilde{x}(k)] = (u_{\mathrm{OGS}}(k) - u_s(k))^2. \tag{17}$$

A similar approach, in which an active control law is approximated by a semiactive suspension by minimizing the square difference between the active and semiactive laws was presented in [1].

Let us first assume that $x_3(k) \neq x_4(k)$; then the value $f^*(k)$ such that $F[f^*(k), \tilde{x}(k)] = 0$ is

$$f^*(k) = -\frac{u_{\mathrm{OGS}}(k) + \lambda_s \left(x_2(k) - x_1(k)\right)}{x_4(k) - x_3(k)} = -\frac{u_{\mathrm{OGS}}(k) + \lambda_s \Delta x(k)}{\Delta v(k)}. \tag{18}$$

where $\Delta x = x_2 - x_1$ is the suspension deformation and $\Delta v = x_4 - x_3$ is its rate of change.

It is easy to see that in this case

$$f(k) = \min_{f \in [f_{\min}, f_{\max}]} \arg F[f, \tilde{x}(k)] = \begin{cases} f_{\max} & \text{if} \quad f^*(k) > f_{\max} \\ f^*(k) & \text{if} \quad f^*(k) \in [f_{\min}, f_{\max}] \\ f_{\min} & \text{if} \quad f^*(k) < f_{\min} \end{cases}. \tag{19}$$

When $x_3(k) = x_4(k)$, regardless of the values of f the damper does not give any contribution to $u_s(k)$. Thus, in this case we assume that if $k > 0$ then $f(k) = f(k-1)$, i.e., the value of the damper coefficient is not updated, while if $k = 0$ we arbitrarily choose $f(0) = f_{\max}$.

We would like now to discuss an interesting point. The OGS law was designed to approximate the optimal target u^*; this procedure ensured that the constraint (12) was always satisfied, i.e., the force u_{OGS} acting on the body of the vehicle does never exceed in magnitude the value $u_{\max}$. In this section, we are discussing a semiactive approximation u_s of the OGS law; in this case, however, the constraint (12) may be violated in some state space regions.

It is possible to prove that, regardless of the value of u_{OGS}, the approximation u_s satisfies constraint (12) if and only if Δx and Δv assume particular values.

Proposition 1. Let $\Delta x = x_2 - x_1$ and $\Delta v = x_4 - x_3$. The relation $|u_s| \leq u_{\max}$ holds if and only if $(\Delta x, \Delta v)$ belongs to one of the following regions.

- Region 1: $\Delta x \in (-\infty, -\frac{u_{\max}}{\lambda_s})$, and $\Delta v \in [-\frac{u_{\max} + \lambda_s \Delta x}{f_{\max}}, \frac{u_{\max} - \lambda_s \Delta x}{f_{\min}}]$.
- Region 2: $\Delta x \in [-\frac{u_{\max}}{\lambda_s}, \frac{u_{\max}}{\lambda_s}]$, and $\Delta v \in [-\frac{u_{\max} + \lambda_s \Delta x}{f_{\min}}, \frac{u_{\max} - \lambda_s \Delta x}{f_{\min}}]$.

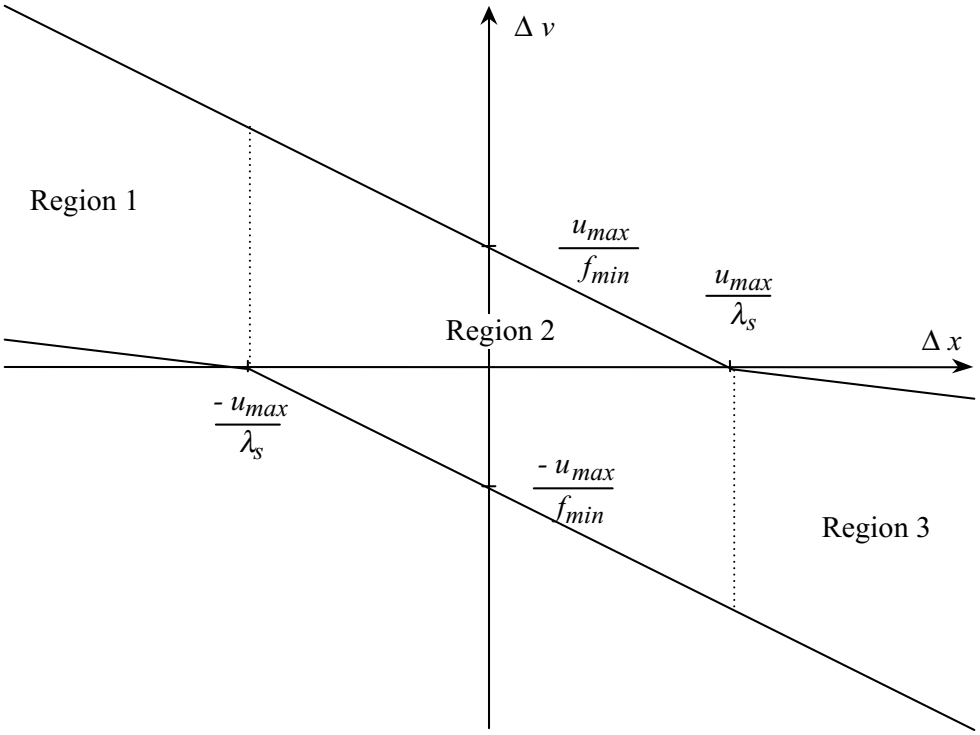

Figure 2: *Regions of the state space defined in Proposition 1.*

- Region 3: $\Delta x \in (\frac{u_{\max}}{\lambda_s}, \infty)$, and $\Delta v \in [-\frac{u_{\max} + \lambda_s \Delta x}{f_{\min}}, \frac{u_{\max} - \lambda_s \Delta x}{f_{\max}}]$.

Proof. Follows from Lemma 2 in appendix. □

The regions defined in the previous proposition can be drawn in the $\Delta x - \Delta v$ plane and are shown in Figure 2.

5 Applicative example

In this section we discuss the results of several simulations. First, however, we explain the choices we have made for the various parameters.

The proposed procedure has been applied to the quarter car suspension shown in Figure 1, with values of the parameters taken from [14]: $M_1 = 28.58$Kg, $M_2 = 288.90$Kg, $\lambda_t = 155900$N/m. The value of $\lambda_s = 14345$N/m has been taken from [2].

To define completely the augmented matrix $\tilde{A}$ it is necessary to assume reference values for α and V. In the following we have taken $\alpha = 0.15\text{m}^{-1}$ and $V = 30\text{m/s}$. These values of α and V have been used in [8] to describe an asphalt road profile. Note that these are nominal design parameters according to which our procedure determines the gain feedbacks for the active control. In the actual simulation the road profile that is creating the disturbance may well be different (e.g., it may correspond to uneven roads as in simulation 2 below).

The control approach we have followed in this paper makes use of a discrete-time state space model. The choice of the sampling interval T needs some warrant. We have assumed $T = 0.01\text{s}$ that is to say a sampling frequency equal to $\omega_s = 2\pi/T \simeq 6 \cdot 10^2\text{rad/s}$. This is essentially due to four important reasons.

- The bandwidth of the passive suspension system described by eq. (1) is $\omega_b < 2 \cdot 10^2\text{rad/s}$. A sampling frequency of $\omega_s \simeq 6 \cdot 10^2\text{rad/s}$ is in good agreement with Shannon's theorem [11] that requires $\omega_s > 2\omega_b$.

- This choice of sampling interval is consistent with eq. (10). In fact, $2\pi \left(\frac{M_1}{\lambda_t}\right)^{1/2} \simeq 8.5 \cdot 10^{-2}\text{s}$ and thus we can be sure that the sampled system will maintain the properties of stabilizability and observability.

- We have observed that an increment in the sampling frequency produces a corresponding increment in the various j_ρ which characterize the linear regions. As j_ρ increases, the time to compute at each step the target control force $u_{OGS}(k)$ also increases. In fact, to determine the value of ρ associated to a given state $\tilde{x}(k)$ we need to compute $Z_\rho \tilde{x}(k)$, where the matrix Z_ρ has $j_\rho + 1$ rows. For the chosen value of T we have that $j_\rho < 100$ for all ρ's, as shown below.

  The clock time of standard microprocessors that may be used to implement such a controller is of the order of 100ns, and since each addition/multiplication requires up to a few clock cycles, we are sure that the sampling time does not imposes any real time constraint.

- To change f the controller must change the opening of the damper valve. Present technology impose a limit of about 10^2Hz on the updating frequency of the damper coefficient.

We have taken $u_{\max} = -u_{\min} = 3000\text{N}$ that is slightly less than the total weight resting

i	1	2	3	4	5	6	7	8	9	10
ρ_i	0.01	0.1	0.5	1	4	20	50	100	1000	10^5
j_{ρ_i}	88	57	46	42	38	36	35	35	35	34

Table 1: *Weight coefficients ρ and relative indices j_ρ.*

on one wheel. A control force of higher magnitude may cause loss of contact between wheel and road. Furthermore, this constraint also limits the acceleration of the sprung mass and this is a necessary condition for the comfort of passengers.

The matrices Q and R, taken from [14] and fitted to the new state space, are:

$$Q = \begin{bmatrix} 11 & -1 & 0 & 0 & 0 \\ -1 & 1 & 0 & 0 & 0 \\ 0 & 0 & 0 & 0 & 0 \\ 0 & 0 & 0 & 0 & 0 \\ 0 & 0 & 0 & 0 & 0 \end{bmatrix} ; \; r = 0.8 \cdot 10^{-9}.$$

These weights, realizing a trade-off between road holding and comfort, lead to a good performance.

Another important aspect of the proposed design procedure deals with the choice of the weighting coefficients $\{\rho_1, \rho_2, \ldots, \rho_m\}$. The weighting coefficient ρ_1 should be determined such that the linear region Γ_{ρ_1} contains all initial conditions of interest. The weighting coefficient ρ_m should be selected such that the region Γ_{ρ_m} covers small disturbances or very small system noises. The other weighting coefficients have been chosen, following Yoshida [16] such that the ratio of the 2-norm for two adjacent gains K_{ρ_i} is $\simeq 1.6 \div 1.8$. We assumed $m = 10$ as it seems a good trade-off between computational efficiency and performance. The chosen values are shown in the table below. It can be noted that in this case j_ρ is a nonincreasing function of ρ.

Finally we have assumed $f_{\min} = 800$Ns/m and $f_{\max} = 3000$Ns/m. From these numerical values we can observe that the regions of the state space defined in Proposition 1 are not very restrictive and the evolution of the system is almost always in region 2. In fact we have: $u_{\max}/\lambda_s \simeq 20$cm and $u_{\max}/f_{\min} \simeq 4$m/s.

To show the performance of our semiactive suspension design, we have simulated three different situations.

5.1 Simulation 1

In the first simulation we considered null initial conditions, i.e., $\tilde{x}(0) = 0$.

We assumed that the only disturbance acting on the system is caused by an asphalt road profile of the same type of the one that was used to derive the augmented matrix $\tilde{A}$. The corresponding parameters, as discussed above, are [8]: $\alpha = 0.15\text{m}^{-1}$, $V = 30\text{m/s}$, e $\sigma = 9\text{mm}^2$.

The results of this simulation are shown in Figure 3.

Figure a) shows the road profile x_0 along with the wheel x_1 and sprung mass x_2 displacement. It is possible to observe that the semiactive suspension filters the high frequencies smoothing the movement of the sprung mass.

Figures b) and c) compare the wheel and sprung mass displacement of the semiactive suspension with that of a completely active one. The two curves are quite similar, that is to say we have not lost in performance by substituting the actuator with the adaptive passive suspension.

Figure d) compares the semiactive control force u_s with the reference active force u^r_{OGS}. The value of u^r_{OGS} at a sampling instant k, is the value of the active force computed by the OGS controller for the given $x(k)$. The two values are different only when f saturates. We also note that u_s is always bounded in magnitude by $u_{\max}$: this is because the evolution in the plane Δx–Δv is always contained in region 2.

Figure e) shows the value of damper coefficient f as a function of time.

It is important to underline that the system evolution is always internal to $\Gamma_{\rho_{10}}$ because the small value of the disturbance does not move the state vector too far from the origin.

5.2 Simulation 2

In the second simulation we considered again zero initial conditions.

We assumed, however, that the disturbance acting on the system be caused by a very rough road profile. Crosby and Karnopp [4, Fig. 10] gave the power spectral density for such an input disturbance. We were able to obtain a similar power spectral density by choosing in eq. (2) the following parameter values: $\alpha = 0.2\text{m}^{-1}$, $\sigma^2 = 0.1\text{m}^2$ and

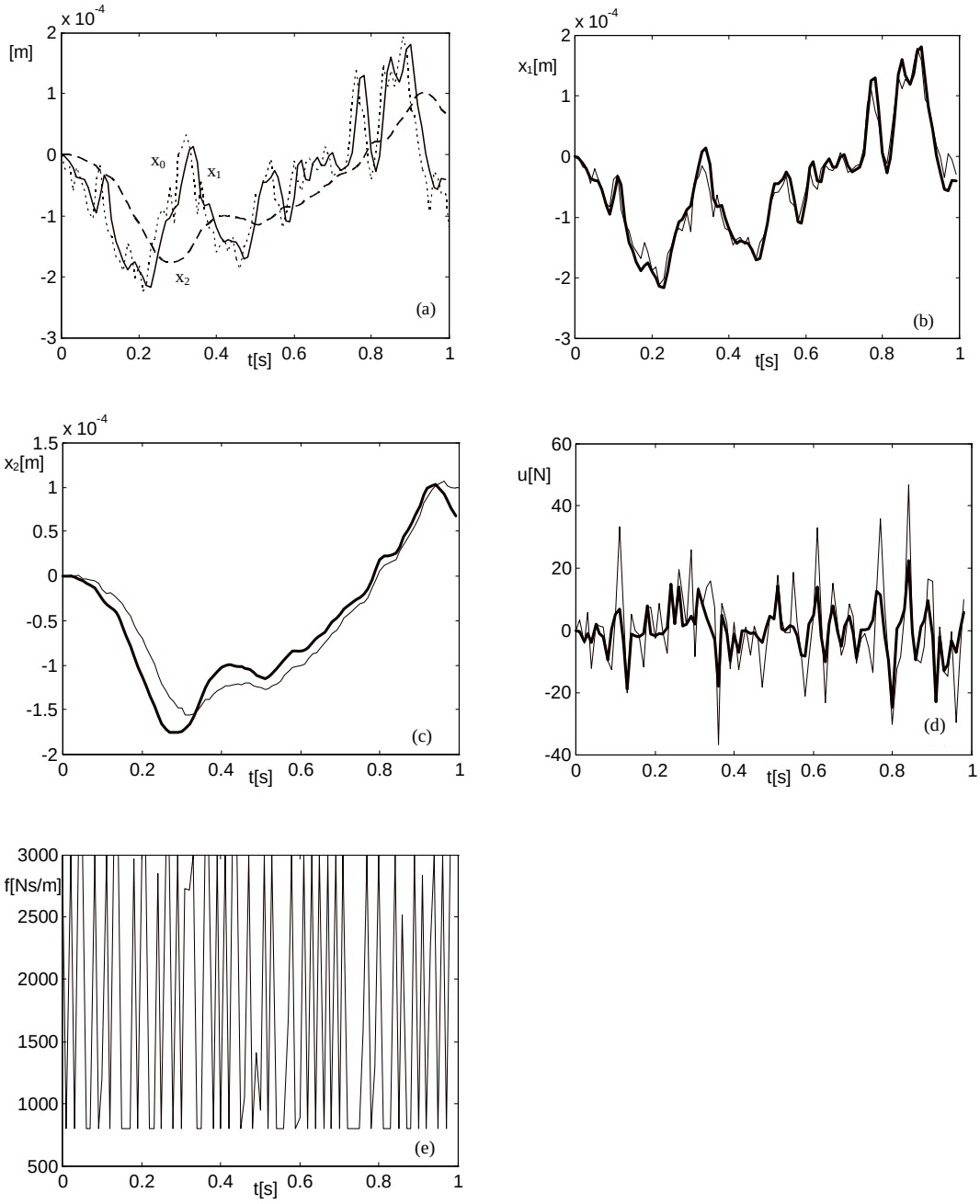

Figure 3: *The results of simulation 1. (a) Evolution of x_0 (dotted), x_1 (continuous) and x_2 (dashed) for the semiactive suspension. (b) Evolution of x_1 for the semiactive (thick) and active (thin) suspension. (c) Evolution of x_2 for the semiactive (thick) and active (thin) suspension. (d) Evolution of semiactive force u_s (thick) and reference active force u^r_{OGS} (thin). (e) Evolution of the damper coefficient f of the semiactive suspension.*

$V = 20\text{m/s}$.

The results of this simulation are shown in Figure 4.

Figures from a) to e) are similar to those of Simulation 1.

Figure f) shows the values of the index i of the linear regions Γ_{ρ_i} as a function of time. The disturbance is sufficiently large to move the state away from $\Gamma_{\rho_{10}}$ although the evolution is always contained within Γ_{ρ_8}.

5.3 Simulation 3

In the third simulation we considered an initial state different from zero and no disturbance. We assumed $\tilde{x}(0) = [\ 0.015 \quad 0.1 \quad 0 \quad 0 \quad 0\ ]^T$.

The results of this simulation are shown in Figure 5.

Figures a) and b) compare the wheel and sprung mass displacement of the semiactive suspension with that of a completely active one. The two curves are quite similar.

Figure c) compares the semiactive control force u_s with the reference active force u^r_{OGS}. Figure d) shows the value of damper coefficient f as a function of time.

Figure e) shows the system evolution in the plane Δx–Δv. We observe that this evolution is contained in region 2 (as defined in Proposition 1). This means that $|u_s|$ never exceeds the value $u_{\max}$, as also shown in Figure c).

Figure f) shows the values of the index i of the linear regions Γ_{ρ_i} as a function of time.

6 Conclusions

This paper presents a two-phase design technique for semiactive suspensions.

In the first phase, a procedure proposed by Yoshida et al. is used to compute a target active control law that can be implemented by Optimal Gain Switching. This control law is such that the force generated by the suspension system is bounded within a set U.

In the second phase, this target is approximated by controlling the damper coefficient of the semiactive suspension. We have also computed the region of the state space in which

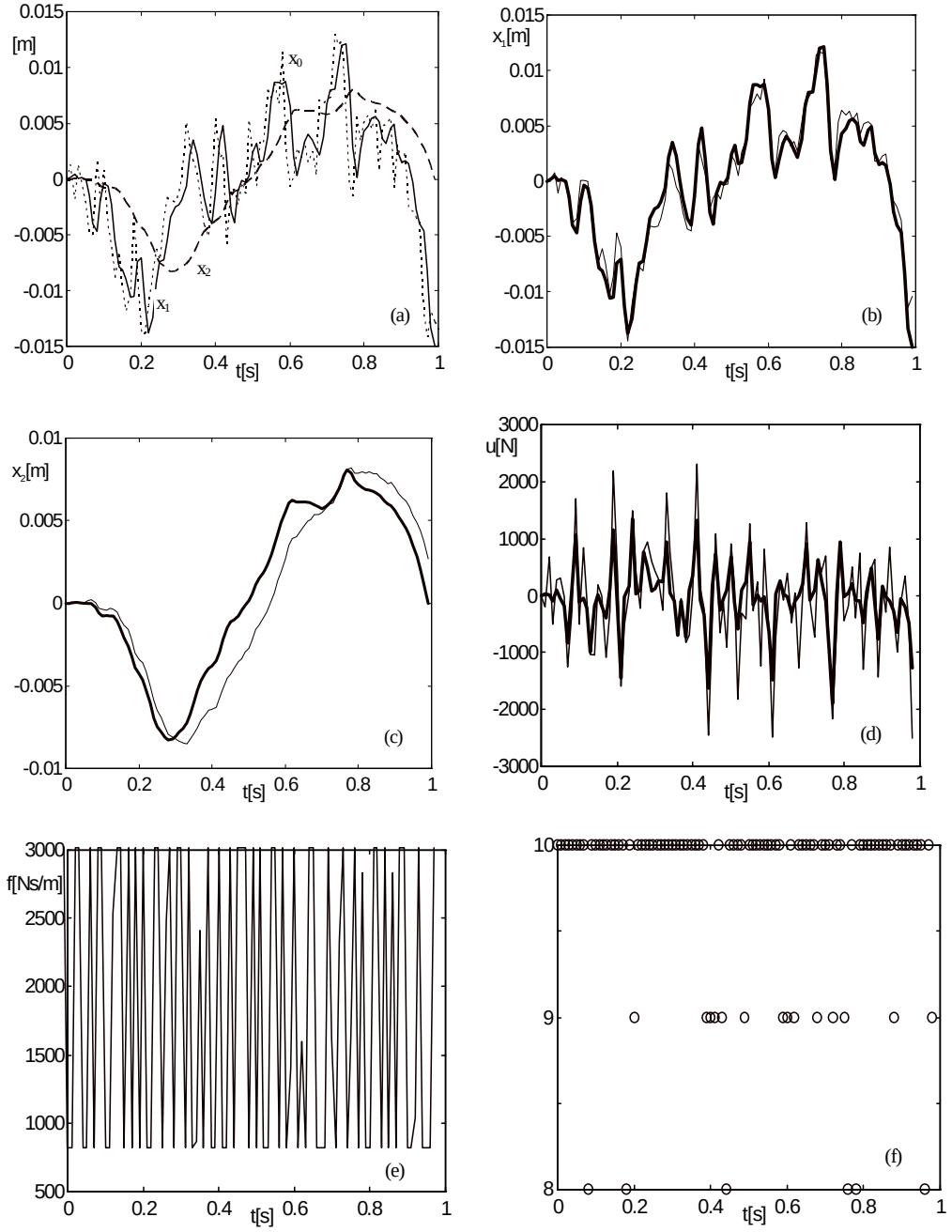

Figure 4: *The results of simulation 2. (a) Evolution of x_0 (dotted), x_1 (continuous) and x_2 (dashed) for the semiactive suspension. (b) Evolution of x_1 for the semiactive (thick) and active (thin) suspension. (c) Evolution of x_2 for the semiactive (thick) and active (thin) suspension. (d) Evolution of semiactive force u_s (thick) and reference active force u^r_{OGS} (thin). (e) Evolution of the damper coefficient f of the semiactive suspension. (f) Values of the index i of the linear regions Γ_{ρ_i} during the evolution of the semiactive suspension.*

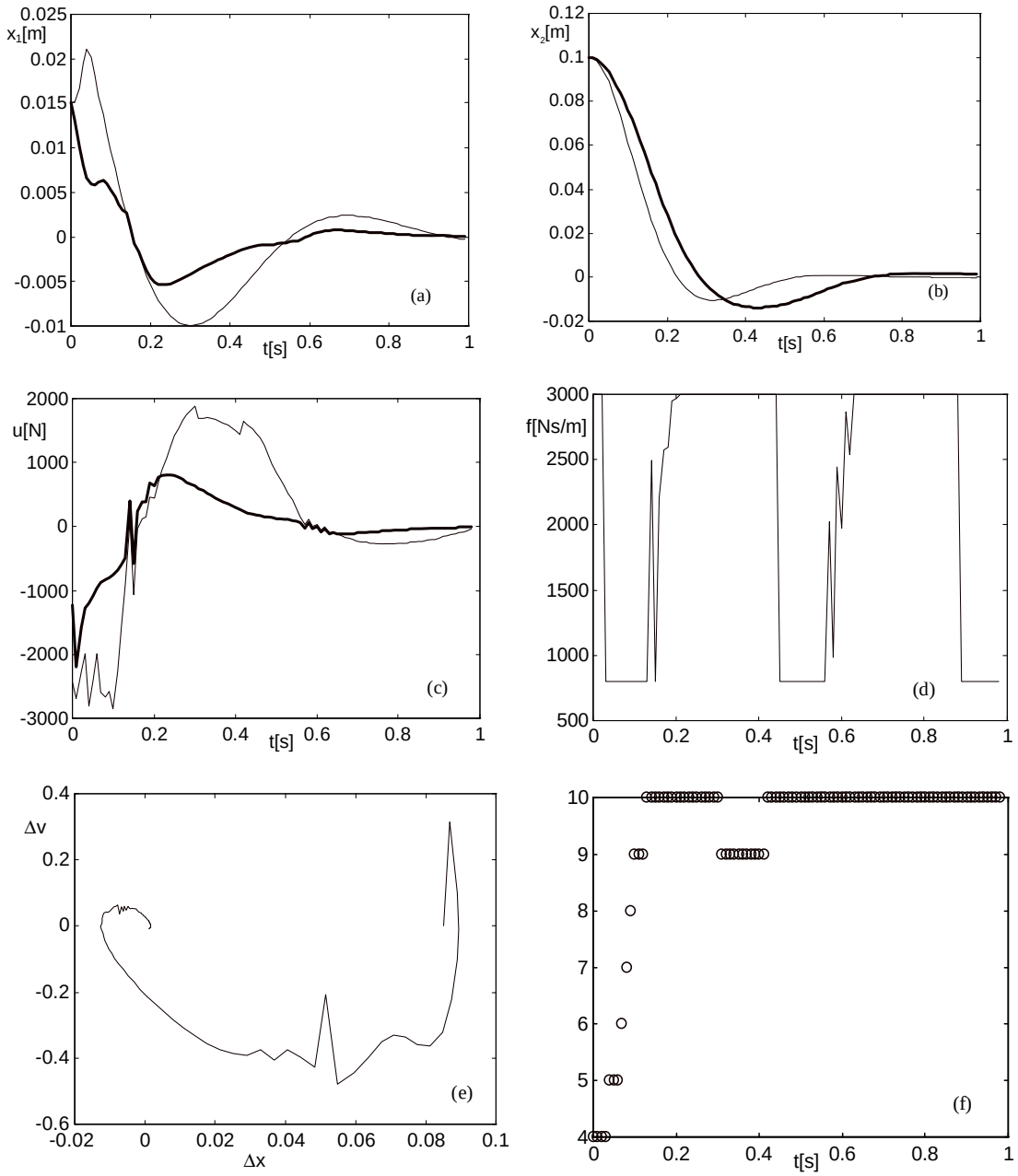

Figure 5: The results of simulation 3. (a) Evolution of x_1 for the semiactive (thick) and active (thin) suspension. (b) Evolution of x_2 for the semiactive (thick) and active (thin) suspension. (c) Evolution of semiactive force u_s (thick) and reference active force u^r_{OGS} (thin). (d) Evolution of the damper coefficient f of the semiactive suspension. (e) System evolution in the Δx–Δv plane. (f) Values of the index i of the linear regions Γ_{ρ_i} during the evolution of the semiactive suspension.

the force generated by the semiactive suspension is ensured to be within the set U.

The results of several simulations have shown that the use of a semiactive suspension leads to minimal loss with respect to the performance of an active OGS suspension.

Appendix

Let us consider a semiactive suspension whose damper coefficient f is adapted so that the suspension force u_s, given by eq. (16), is as close as possible to a reference active force u. This can be done with the procedure outlined in eqs. (18) (19) where we set $u_{OGS} = u$.

We assume that $u \in U$, where $U = [u_{\min}, u_{\max}]$. We also assume that $f \in [f_{\min}, f_{\max}]$. The following lemma gives necessary and sufficient conditions for u_s to belong to the set U as well. This is done by finding suitable constraint sets for the evolution of the suspension deformation $\Delta x = x_2 - x_1$ and of its velocity $\Delta v = x_4 - x_3$.

Lemma 2. The relation $u_s \in U$ holds if and only if $(\Delta x, \Delta v)$ belongs to one of the following regions.

- Region 1: $\Delta x \in (-\infty, -\frac{u_{\max}}{\lambda_s})$, and $\Delta v \in [-\frac{u_{\max} + \lambda_s \Delta x}{f_{\max}}, -\frac{u_{\min} + \lambda_s \Delta x}{f_{\min}}]$.
- Region 2: $\Delta x \in [-\frac{u_{\max}}{\lambda_s}, -\frac{u_{\min}}{\lambda_s}]$, and $\Delta v \in [-\frac{u_{\max} + \lambda_s \Delta x}{f_{\min}}, -\frac{u_{\min} + \lambda_s \Delta x}{f_{\min}}]$.
- Region 3: $\Delta x \in (-\frac{u_{\min}}{\lambda_s}, +\infty)$, and $\Delta v \in [-\frac{u_{\max} + \lambda_s \Delta x}{f_{\min}}, -\frac{u_{\min} + \lambda_s \Delta x}{f_{\max}}]$.

Proof. We will give a geometrical proof relative to the case $\Delta x \lambda_s \leq u_{\min}$ that corresponds to region 1. The proofs for the other cases can be derived with a similar reasoning.

Let us consider Figure 6. The thick line represents the generic curve $f^*(u)$ — as given by (18) setting $u_{OGS} = u$ — for a given value of Δx and Δv. The striped segment on the horizontal axis represents the domain of u_s for the line f^* considered, as u ranges in U.

If $-\Delta x \lambda_s \leq u_{\min}$, the intersection $-\lambda_s \Delta x$ of f^* with the horizontal axis lies on the left of $u_{\min}$. The dashed lines s_1 and s_2 — passing through points A and D, respectively — correspond to the extreme values of Δv in region 1 for the chosen value of Δx, i.e., line s_1 corresponds to $\Delta v = -(u_{\min} + \lambda_s \Delta x)/f_{\max}$, while line s_2 corresponds to $\Delta v = -(u_{\max} + \lambda_s \Delta x)/f_{\min}$. Thus, the generic line f^* for $\Delta x, \Delta v$ in region 1 must be contained within the cone defined by lines s_1 and s_2.

1. We first prove that all lines f^* that are not within the cone $s_1 - s_2$ lead to values of u_s not in U.

   (a) Let us consider a line f^* within the cone $r - s_1$. For all values of u in U, f saturates at the value $f_{\max}$ and this leads to $u_s < u_{\min}$.

   (b) Let us consider a line f^* within the cone defined by s_2 and the positive real axis. For all values of u in U, f saturates at the value $f_{\min}$ and this leads to $u_s > u_{\max}$.

   (c) Let us consider a line f^* with a negative slope. For all values of u in U, f saturates at the value $f_{\min}$ and this leads to $u_s < u_{\min}$.

2. Secondly, we prove that for all lines f^* that are within the cone $s_1 - s_2$ the condition $u_s \in U$ can never be violated. We observe, in fact, that the condition can only be violated when $u_s \neq u$, i.e., when f is in saturation and thus takes either the value $f_{\min}$ or $f_{\max}$. Let us consider a generic line f^* within this cone.

   (a) If the line f^* intersects the segment A-B, then there exist values of u in U such that f saturates at $f_{\max}$ but the saturation leads to values of $u_s \in U$. If the line does not intersect the segment A-B, then for all values of u in U, f cannot saturate at $f_{\max}$.

   (b) If the line f^* intersects the segment C-D, then there exist values of u in U such that f saturates at $f_{\min}$ but the saturation leads to values of $u_s \in U$. If the line does not intersect the segment C-D, then for all values of u in U, f cannot saturate at $f_{\min}$.

   We have proved that for all lines f^* within the cone $s_1 - s_2$, if f saturates then $u_s \in U$, hence condition (12) can never be violated.

A similar construction can be drawn for the case $-\Delta x \lambda_s \in U$. In this case the intersection of the line f^* with the horizontal axis lies within U, and the two lines s_1 and s_2 that delimit region 2 pass through points C and D, respectively.

A similar construction can be drawn for the case $-\Delta x \lambda_s > u_{\max}$. In this case the intersection of the line f^* with the horizontal axis lies on the right of $u_{\max}$, and the two lines s_1 and s_2 that delimit region 3 pass through points C and B, respectively.

□

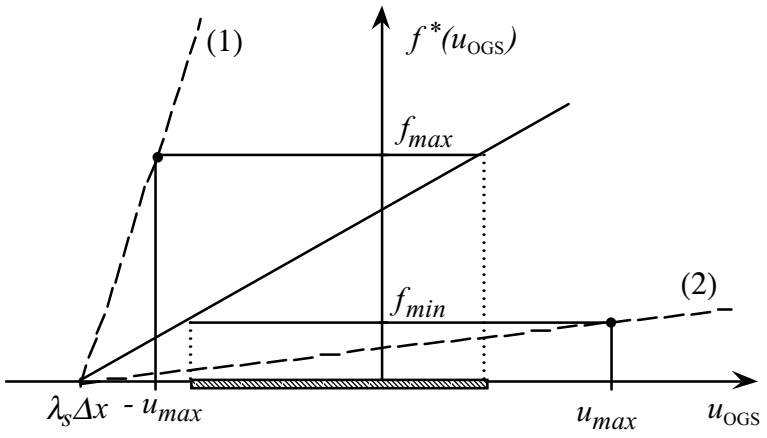

Figure 6: *Geometrical construction corresponding to region 3.*

References

[1] Cheok, K.C., Loh, N.K., McGree, H.D. and Petit, T.F.: Optimal model following suspension with microcomputerized damping. IEEE Trans. on Industrial Electronics, Vol. 32, No. 4, November 1985.

[2] Corriga, G., Giua, A. and Usai G.: An H_2 formulation for the desing of a passive vibration-isolation system for cars, Vehicle System Dynamics, Vol. 26, pp. 381–393, 1996.

[3] Corriga, G., Sanna, S. and Usai G.: An optimal tandem active-passive suspension for road vehicles with minimum power consumption. IEEE Trans. on Industrial Electronics, Vol. 38, No. 3, pp. 210–216, 1991.

[4] Crosby, M.J. and Karnopp, D.C.: The active damper: a new concept in shock and vibration control. 43rd Shock and Vibration Bulletin, June 1973.

[5] Giua, A., Savastano, A., Seatzu, C. and Usai G.: Tandem Active-Passive Suspension Design with Constraints on the Forces. Proc. Int. Conf. on Advances in Vehicle Control and Safety (Amiens, France), July 1998.

[6] Göring, E., von Glasner, E.C., Povel, R. and Schützner P.: Intelligent suspension systems for commercial vehicles. Proc. Int. Cong. MV2, Active Control in Mechanical Engineering (Lyon, France), pp. 1–12, June 1993.

[7] Grima, M. and Renou C.: Modelization of semiactive suspensions. Proc. Int. Cong. MV2, Active Control in Mechanical Engineering (Lyon, France), Vol. 1, June 1993, (in French).

[8] Hac, A.: Suspension optimisation of a 2-DOF vehicle model using a stochastic optimal control technique. Journal of Sound and Vibration, Vol. 100, No. 3, pp. 343–357, 1985.

[9] Krasnicki, E. J.: Comparison of analytical and experimental results for a semi-active vibration isolator. The Shock and Vibration Bulletin, pt. 4, pp. 69–76, September 1980.

[10] Kwakernaak, H. and Sivan R.: Linear Optimal Control Systems. Wiley Interscience (New York), 1972.

[11] Ogata, K.: Discrete-time control systems. Prentice Hall International Editions, 1972.

[12] Roberti, V., Ouyahia, B. and Devallet A.: Oleopneumatic suspension with preview semi-active control law. Proc. Int. Cong. MV2, Active Control in Mechanical Engineering (Lyon, France), Vol. 1, June 1993.

[13] Savastano, A.: Synthesis of a Optimal Gain Switching controller for linear discrete-time systems with constrained input: application to an active suspension system for cars. Laurea Thesis, Dept. of Electrical and Electronic Eng., University of Cagliari (Italy), 1997, (in Italian).

[14] Thompson, A.G.: An active suspension with optimal linear state feedback. Vehicle System Dynamics, Vol. 5, pp. 187–203, 1976.

[15] Wonham, W.M. and Johnson C.D.: Optimal bang-bang control with quadratic performance index. Trans. ASME Journal of Basic Engineering, Vol. 86, pp. 107–115, March 1964.

[16] Yoshida, K., Nishimura Y. and Yonezawa Y.: Variable gain feedback for linear sampled-data systems with bounded control. Control Theory and Advanced Technology, Vol. 2, No. 2, pp. 313–323, June 1986.